Impacts of Soil Moisture Ocean Salinity (SMOS) Soil Moisture Initialization on Convection Forecasting in the U.S. Great Plains

Thomas W. Collow[1] and Alan Robock

Department of Environmental Sciences, Rutgers University, New Brunswick, NJ

Wei Wu

Biological, Environmental & Climate Sciences Department, Brookhaven National Laboratory, Upton, NY

Submitted to *Journal of Geophysical Research Atmospheres*

August, 2014

Corresponding Author:
Thomas W. Collow
INNOVIM, LLC
NOAA/NWS/NCEP Climate Prediction Center
5830 University Research Court
College Park, MD 20740
Phone: 301-683-3464
E-mail: thomas.collow@noaa.gov

1. Now at INNOVIM, LLC., NOAA/NWS/NCEP/Climate Prediction Center, College Park, MD

Abstract

The sensitivity of short term forecasts of precipitation, temperature, and dewpoint to soil moisture initialization in the Weather Research and Forecasting (WRF) model was investigated. Model simulations were initialized with soil moisture values from the North American Regional Reanalysis (NARR) dataset and with those retrieved from the Soil Moisture Ocean Salinity (SMOS) satellite. SMOS soil moisture data were bias-corrected based on a 2 year soil moisture climatology difference between NARR and SMOS before being regridded and directly inserted into the model. The insertion method was simplistic with no cycling between days. In addition, runs which applied a 0.10 m^3/m^3 soil moisture addition for each scenario to account for the observed NARR bias were performed. Ten cases were chosen which met the criteria of having convection, but with minimal synoptic-scale forcing, and having a SMOS pass covering the Great Plains region. Results showed minimal changes in precipitation forecast skill in all of the runs, but there was a more substantial relationship between the initial soil moisture changes and the modeled 2 m temperature and dewpoint changes. WRF runs with the SMOS soil moisture configuration significantly improved forecasts of maximum temperature and dewpoint when compared to Oklahoma Mesonet observations for some cases. These results using SMOS soil moisture showed some promise in terms of the usefulness of the satellite data, but given the simplicity of the insertion method, more work will need to be done with sophisticated data assimilation techniques to confirm these results.

1. Introduction

This study performs a simplistic substitution of Soil Moisture Ocean Salinity (SMOS) soil moisture products into the Advanced Research Core of the Weather Research and Forecasting Model (WRF) [*Skamarock*, 2008], using 4 km horizontal resolution integrations with explicit treatment of convection. The goal is to assess the sensitivity of initial soil moisture to daytime temperature, dewpoint, and convective precipitation. Previous studies [e.g., *Done et al.*, 2004; *Weisman et al.*, 2008] found a more realistic diagnosis of convection using such runs compared to coarser models, which are subject to convective parameterizations that may contain errors. *Kain et al.* [2008] concluded no increase in skill from using a 2 km horizontal resolution over a 4 km horizontal resolution and given the increased computing power required for higher resolution runs, 4 km runs were decided as optimal. Given the coupling that exists between the land surface and atmosphere, it is important to assess the ability of models to accurately depict known relationships between soil moisture, temperature, dewpoint, and precipitation. Data assimilation experiments attempt to adjust the initial soil moisture to an optimal level based on observed and modeled data. Because of this, it is necessary to assess both the validity of the modeled data and the sensitivity of the model to soil moisture changes.

Several studies have found a strong relationship between soil moisture changes and resultant impacts on convective development. *Pielke and Zeng* [1989] found that wetting soil through irrigation can increase the probability of convective development. *Trier et al.* [2004] used a high-resolution initialization of soil moisture and noted more accurate convection initialization compared to when a lower resolution initial soil moisture data set was used. Studies by *Lanicci et al.* [1987], *Mahfouf et al.* [1987], *Chang and Wetzel* [1991], *Clark and Arrit* [1995], *Frye and Mote* [2010], and *Case et al.* [2011] all show soil moisture having some

impact on convective development or mesoscale circulations. *Ookouchi et al.* [1984] found that soil moisture boundaries can create mesoscale circulations similar to summertime sea breezes, which could drive convection. While *Collow et al.* [2014] did not find any major changes in convective precipitation due to soil moisture changes, only uniform soil moisture changes were made in cases with extreme synoptic forcing. This study imposes non-uniform adjustments based on SMOS values for cases with weaker forcing, specifically where no dryline or low level jet stream was present to force convection. Given the numerous soil moisture remote sensing projects in progress including Advanced Microwave Scanning Radiometer 2 (AMSR2) [*Imaoka et al.*, 2010], Argentine Microwaves Observation Satellite (SAOCOM; http://www.invap.com.ar/en/projects/saocom-satellites.html), and Soil Moisture Active Passive (SMAP) [*Entekhabi et al*., 2010], it is important to assess the potential uses and applications of the data provided by these programs. While this study is not intended to directly assess the usefulness of SMOS soil moisture data assimilation due to limitations in the methodology, it will provide an assessment of WRF sensitivity to changed spatial soil moisture and allow a determination of the potential of SMOS to be used for such experiments.

The SMOS satellite was launched in 2009 by the European Space Agency and is designed to infer soil moisture content through measurements of brightness temperature from an L-band radiometer. The wavelength at which SMOS observes is considered ideal for soil moisture measurements [*Vinnikov et al.*, 1999; *Njoku et al*., 2003] as shorter wavelengths (higher frequencies) are more sensitive to errors resulting from the effects of vegetation and surface roughness, while longer wavelengths (lower frequencies) are more susceptible to interference from anthropogenic radio waves. SMOS has a horizontal resolution of approximately 40 km and a mission objective of soil moisture measurement accuracy within 0.04 m^3/m^3 [*Kerr et al.*, 2001].

Several studies have evaluated SMOS soil moisture products against in-situ soil moisture observations. *Bitar et al.* [2012], using Soil Climate Analysis Network observations over the continental United States, and *Collow et al.* [2012], focusing on the United States Great Plains and using a variety of in situ sensors over a single SMOS footprint, both found that SMOS soil moisture retrievals were too dry. *Jackson et al.* [2012] looked at four individual watersheds over different regions of the United States, each having different soil types, and found that the SMOS errors were close to the target accuracy of 0.04 m^3/m^3. The difficulty in measuring coarse-scale soil moisture from ground-based sensors was highlighted by *Collow et al.* [2012], who showed large differences in soil moisture values even among sensors close in proximity to each other, which could be explained by different sensor calibration methods and the high spatial variability of soil moisture. Because of this spatial variability, *Crow et al.* [2012] concluded that is infeasible to compare an entire footprint to a single point observation. Although the actual soil moisture values may be questionable, the aforementioned evaluation studies show a good temporal correlation between the SMOS data and in-situ observations indicating their potential usefulness. SMOS soil moisture is beginning to be ingested into weather forecasting models, most notably at the European Center for Medium Range Weather Forecasting (ECMWF) [*Sabater et al*., 2012]. *Schneider et al.* [2013] assimilated soil moisture from the Advanced Scatterometer (ASCAT) and saw improvements in convection forecasts in a regional model. Using an offline land surface model, *Draper et al.* [2012] found that the assimilation of soil moisture products from ASCAT and the Advanced Microwave Sounding Radiometer (AMSR-E) improved modeled soil moisture when compared to in-situ observations.

Here the goal will be to assess whether or not a simple SMOS soil moisture substitution can improve weather forecasts. If it indeed does so, then it can only be expected that more

130 complex data assimilation systems [e.g., *Reichle,* 2008] will improve forecasts even more
131 signifying the potential usefulness of the satellite data. However, even if no improvements are
132 found using the simplistic approach in this experiment, it is still possible that more traditional
133 data assimilation procedures would still create improvements, as they would create an optimal
134 blend of the model and satellite observations, rather than our approach which just treats the
135 observations as 100% truth. *Zhao et al*. [2014] showed that data assimilation of SMOS soil
136 moisture into a land surface model resulted in more accurate soil moisture compared to just
137 remotely sensed data and open loop simulations over the Tibetan Plateau. We seek to determine
138 the potential usefulness of SMOS soil moisture data with the absolute minimum of what would
139 be required to conduct a data assimilation experiment. Therefore, any positive results from this
140 experiment could be used to show that more robust data assimilation experiments using SMOS
141 will likely further improve forecasts.

142 **2. Model Set-Up**

143 **2.1 Basic Configuration**

144 The model used in this study is version 3.4.1 of the Advanced Research core of the WRF
145 model (WRF-ARW). The nesting and parameterization schemes are identical to those used in
146 the base configuration from *Collow et al.* [2014]. As in that study, WRF schemes were chosen to
147 mimic the configuration of the National Oceanic and Atmospheric Administration Storm
148 Prediction Center. The microphysics, longwave radiation, shortwave radiation, and planetary
149 boundary layer schemes used were the WRF Single Moment 6 Class Microphysics Scheme
150 [*Hong and Lim*, 2006], the Rapid Radiative Transfer Model [*Mlawer,* 1997], the Dudhia Scheme
151 [*Dudhia,* 1989], and the Mellor-Yamada-Janjic (MYJ) scheme [*Mellor and Yamada*, 1982]
152 respectively. A three way nesting was established with the innermost nest having a 4 km

153 horizontal resolution and being focused over the United States Great Plains (429x336 x-y grid),
154 which is shown in Figure 1. This innermost nest has a high enough resolution for convection to
155 be treated explicitly, and is the region where the results will be analyzed. The model was
156 initialized at 00 UTC and run for 30 hours for each of the cases, which are discussed at the end
157 of this section. North American Regional Reanalysis (NARR) [*Mesinger et al.*, 2006] data were
158 used as initial and boundary conditions and WRF was coupled with the Noah Land Surface
159 Model [*Ek et al.*, 2003], which is the same land surface model used in NARR. The horizontal
160 resolution of NARR is approximately 32 km. Because of this relatively low resolution, outer
161 nests were required to force the model but were not used in the evaluation of results. Although a
162 large model domain was used, model output changes may be partially constrained by the
163 constant boundary conditions. However, because of the computing time required to do larger
164 domain runs combined with the success of *Collow et al*. [2014] in producing significant
165 precipitation changes in some analyses within the same domain set-up, the size of the domain is
166 justified.

167 **2.2 SMOS Soil Moisture Substitution**

168 **2.2.1 Regridding to a 4 km Grid**

169 Instead of imposing spatially uniform changes to soil moisture, soil moisture values were
170 adjusted based on measurements from SMOS. Version 5.00 of the SMOS reprocessed dataset
171 was used, which further improved the algorithms used to deduce soil moisture values from native
172 brightness temperature fields and factored out radio frequency interference
173 (https://earth.esa.int/c/document_library/get_file?folderId=127856&name=DLFE-2302.pdf). The
174 level 2 product was used, which is generated at a 15 km horizontal resolution (SMOS level 2
175 processor soil moisture ATBD available online at https://earth.esa.int/pub/ESA_DOC/SO-TN-

ARR-L2PP-0037_ATBD_v3_3.pdf) and individual pixels were close enough so that the data could be regridded to a 4 km resolution to be used in this experiment. The regridding was done using a Cressman Objective Analysis and data were mapped to the grid of the innermost WRF nest. Some pixels are likely to be erroneous as SMOS was not designed for high-resolution modeling. The SMOS data were simply used as a proxy for the soil moisture changes to determine if and how the model would respond and whether or not the data have potential if a more complex data assimilation system was used which would likely result in less errors. Figure 2 illustrates the regridding procedure by showing the locations of each individual pixel and the regridded result for the SMOS pass on 23 June 2010 00 UTC.

2.2.2 Correcting for SMOS Bias

A simple bias correction was then applied to the SMOS data before substitution. Satellite data need to be corrected for biases before being used [*Reichle and Koster*, 2004] in data assimilation experiments and therefore bias correction was applied here as well. In this study, bias was defined as the mean difference between NARR and SMOS over a two year period. Specifically, SMOS data were regridded as described above and compared to NARR data from the non-winter months (March through November) of 2010 and 2011, also regridded to a 4 km grid. The winter season was eliminated as snow cover interferes with the satellite retrievals. Figure 3 shows the mean SMOS soil moisture values, the mean NARR soil moisture values, and the difference between the two at each grid point, which effectively represents the SMOS bias. Elevation data from GTOPO30 [*Gesch et al.*, 1999] is also plotted. GTOPO30 is a high resolution digital elevation model with a horizontal grid spacing of approximately 1 km. There are relatively low soil moisture biases over the Great Plains and larger biases over the Rocky Mountain region in the west. One must take the values over the mountains with caution as

heterogeneities in topography likely result in high soil moisture variability within individual pixels [*Charpentier and Groffman,* 1992]. There are also higher biases further east over Arkansas and Missouri where the land is more forested. Over the domain of interest, where the land use type is mainly grassland and cropland, the biases are closer to zero.

This SMOS bias was removed from the raw SMOS data and then substituted into the WRF model for the surface soil moisture layer (0-10 cm depth). The soil porosity was set as the upper bound for soil moisture, and the same changes that were applied to the surface were applied uniformly to the deeper soil layers (10-40 cm depth, 40-100 cm depth, and 100-200 cm depth) as done by *Collow et al.* [2014]. A greater volume of water was added to the deeper layers due to their increased thickness. Although this may be unrealistic as lower soil layers have less temporal variability than near surface soil moisture, a constant ratio of water to soil was preserved for the changes at all levels. Root zone soil moisture is important, as highlighted by *Sabater et al*. [2006], *Kumar et al.* [2009] and *Draper et al.* [2012], especially in forested environments where the roots grow deeper, and as a result can transport deep water up to the surface. If SMOS data were missing or undefined, the NARR data were not changed. Using this method, a new soil moisture initialization dataset was generated with non-uniform changes.

2.3 Summary of Simulations

Since the model runs start at 00 UTC, descending SMOS passes were used, which measure soil moisture over the Great Plains at approximately the same time. The runs used identical initial conditions except for soil moisture. The soil moisture configurations were the original NARR (CONTROL-Run), NARR substituted with bias corrected SMOS as previously explained (SMOS-Run), and two additional runs that add 0.10 m^3/m^3 to the original NARR (CONTROL + 0.10-Run) and bias corrected SMOS (SMOS + 0.10-Run), as *Collow et al.* [2014]

found that NARR soil moisture data were too dry when compared to Oklahoma Mesonet soil moisture observations. The 0.10 m^3/m^3 addition was applied to all soil levels as described above.

2.4 Cases

Cases were chosen for the years 2010 and 2011 based on several factors outlined below:

1. Occurring during the months of meteorological summer (June through August).
2. Minimal dynamical forcing for convection (no dryline or low level jet stream present).
3. Having at least 1 mm of mean precipitation over an evaluation domain that encompasses Kansas and Oklahoma (Figure 2) calculated using the National Centers for Environmental Prediction (NCEP) Stage IV Precipitation Product [*Lin and Mitchell,* 2005]. The NCEP Stage IV product is derived using radar and gauge data and has undergone some quality control. The 1 mm threshold was chosen arbitrarily based on comparisons with other precipitation thresholds that were tested. A greater threshold would result in fewer useable cases while a reduced threshold would result in more cases but too little precipitation coverage.
4. A SMOS pass covering the evaluation domain at 00 UTC. The swath must cover the entire inner domain region, as opposed to only a fraction. Although SMOS has a revisit time of three days, an appropriate pass will not necessarily occur every three days due to different orientations of the swath. The size of the inner domain is chosen because it is close to the width of a SMOS swath. Using the entire d03 domain would be infeasible as the swath would only cover it partially.

Because of these restrictions only a small number of suitable cases were identified from 2010 and 2011. To be more specific, out of the 184 days available, only 28 had useable SMOS data and 80 had mean precipitation of at least 1 mm in the evaluation domain. There were only ten

days where both of these conditions were met and are selected as cases for this study, namely 23 June 2010, 6 July 2010, 11 July 2010, 24 July 2010, 16 August 2010, 10 June 2011, 28 June 2011, 29 July 2011, 3 August 2011, and 16 August 2011. Model precipitation output was evaluated from 18 UTC to 06 UTC the next day using the NCEP Stage IV product, which covers the afternoon convective development. 2 m Temperature and Dewpoint responses were also assessed.

3. Results

3.1 Precipitation

Precipitation was evaluated using two methods. First a simple areal average of total precipitation across the evaluation domain was applied for each run. Next an analysis of the equitable threat score (*ETS*) was performed to assess the skill of WRF to predict precipitation timing. Table 1 shows precipitation values for all cases and soil moisture scenarios. Figure 4 illustrates the initial soil moisture used in WRF for the four runs beginning 23 June 2010 00 UTC. Both SMOS-Run and CONTROL-Run have the wettest soil across northern Kansas. SMOS-Run has a larger region of drier soil in central and southern Kansas than in CONTROL-Run. There is also a slight increase in soil moisture across southern Oklahoma in SMOS-Run. The gradients of soil moisture are also different. Figure 5 shows the total precipitation output from WRF for each soil moisture configuration and it is easily seen that there are no major differences. While there are subtle differences in location and intensity in each run, there is no clear pattern observed that would indicate the changed soil moisture has a significant impact. These results are consistent for all of the cases. Even for the two cases that the control WRF soil moisture did not resolve precipitation accurately (11 July 2010 and 16 August 2011), the use of SMOS soil moisture did not improve the precipitation forecasts.

Using *ETS*, the ability of WRF to diagnose hourly precipitation patterns was evaluated. *ETS* is calculated based on the number of hits and misses from the model and observations. Here a hit is defined as having any amount of precipitation within a particular grid cell and a miss as having no precipitation in a grid cell.

$$ETS = \frac{a - r}{a + b + c - r}$$

In the equation above a represents the number of grid cells where both the model and observations have a hit, b signifies the number of grid cells with a model hit and an observation miss, and c denotes grid cells with a model miss and observation hit. The number of correct forecasts by chance (r) is determined using the relationship below where n is the sample size, or in this case, the total number of grid points.

$$r = \frac{(a + b)(a + c)}{n}$$

Figure 6 presents the *ETS* for all of the cases and shows that there is little change in skill among the forecasts with different soil moisture initializations. Low skill is generally found for all cases and this agrees with *Weisman et al.* [1997]. At times the *ETS* drops below zero, which indicates better forecast skill from a random forecast than the actual forecast. Figure 7 presents the average *ETS* over all the cases with varying precipitation thresholds for hits and misses. For lower thresholds the mean *ETS* is slightly higher in the increased soil moisture runs. However, the spread is so large that it was impossible to judge the significance. The *ETS* of the SMOS-Run and SMOS + 0.10-Run became greater than CONTROL-Run and CONTROL + 0.10-Run respectively once the hit or miss precipitation threshold reached about 10 mm but once again due to the large spread, the significance was unclear. Also the relationship is not consentient among all cases. Therefore, at this time all that could be concluded is that such land surface changes do

not appear to substantially impact the low precipitation forecast skill at a high horizontal resolution.

3.2 2 m Temperature and Dewpoint

Although one could argue that the results found with precipitation may simply indicate that the model is insensitive to soil moisture changes, other meteorological variables showed more of a response to the changed soil moisture. Spatial correlations were calculated using the initial soil moisture and the resultant maximum and mean temperatures between 18 UTC and 06 UTC the next day at each individual grid cell. It was expected that an increase in soil moisture would create cooling, as more shortwave radiation would be used to evaporate surface water than to heat the surface. Because precipitation can increase the soil moisture, which would therefore impact temperature independently of the initial soil moisture, WRF grid cells with any precipitation throughout the model run were filtered out to allow for a better analysis between the initial soil moisture and 2 m temperature. Table 2 shows the spatial correlation values between the initial soil moisture changes and the maximum and mean 2 m temperature and dewpoint. In terms of temperature, there is a strong spatial anti-correlation between the initial soil moisture and max 2 m temperature with slightly weaker spatial correlations for the 2 m mean temperature. The standard deviation is also higher for the 2 m mean temperature as well.

Figure 8 presents the soil moisture and 2 m temperature differences in addition to a scatterplot for the 23 June 2010 case. The substantial decrease in soil moisture in eastern Kansas is accompanied by warmer temperatures while increased soil moisture in western Kansas resulted in cooler temperatures. The Oklahoma Mesonet provides an archive of past temperature data that are freely available (http://www.mesonet.org/index.php/weather/ mesonet_data_files). For each of the 120 stations, the closest WRF grid cell was found and a comparison was made

between the maximum 2 m temperature from WRF and that found at the Oklahoma Mesonet Station. The goal was to determine whether or not using SMOS soil moisture data created better temperature and dewpoint forecasts despite the minimal impacts on precipitation. Precipitation grid cells and Mesonet sites with precipitation were filtered out over the modeled time period to remove the effects of precipitation on temperature. Table 3 shows the max and mean temperature biases of the WRF model configured with different soil moistures compared to the Mesonet observations. The 6 July 2010 case was discarded from this analysis because of the large areal coverage in precipitation across Oklahoma which would have impacted temperatures in addition to soil moisture as explained above. Results showed that for the remaining cases, the soil moisture addition impacted the mean temperature bias to a similar degree. A t-test was applied to the set of biases for each individual station for each model run. Both CONTROL + 0.10-Run and SMOS + 0.10-Run produced differences in biases that were significant at a 95% confidence interval with respect to runs with no soil moisture change. In four of the cases SMOS-Run mean maximum temperature biases were significantly different from CONTROL-Run with improvements in two of them. In terms of the mean temperature, the significant improvement was seen for 3 out of the 4 cases. The same analysis was repeated for 2 m dewpoint temperatures with similar results. Positive spatial correlations were to be expected as in increase in soil moisture would lead to an increase in low level humidity. This is indeed what was found in WRF. However, the magnitude of the spatial correlations was weaker than that for the temperature correlations. Also, unlike with 2 meter temperatures, the highest correlations were seen with the mean 2 m dewpoint rather than the maximum 2 m dewpoint (Table 2). The standard deviation was also higher for the maximum dewpoint than the mean dewpoint. This suggests that the initial soil moisture influences the dewpoint over a longer time period than the

334 temperature but the overall maximum temperature will be more strongly influenced by initial soil
335 moisture. Table 4 outlines the max and mean dewpoint biases for each of the cases with respect
336 to Mesonet observations. SMOS-Run max dewpoint mean bias was significantly different from
337 CONTROL-Run in 3 cases, in which both were improved. When the average dewpoint was
338 looked at, improvements occurred in 3 of the 4 cases with significant differences. However, like
339 with temperatures, increasing soil moisture did not always improve the forecasts, with the 29
340 July 2011 case as a good example.

341 **4. Discussion and Conclusion**

342 In all but two of the cases, adding 0.10 m^3/m^3 to soil moisture resulted in slightly more
343 areal mean total precipitation and this was true for both CONTROL + 0.10-Run and SMOS +
344 0.10-Run. *Collow et al.* [2014] used a set of model ensembles created using different boundary
345 layer and microphysics schemes, finding that the precipitation differences in the increased soil
346 moisture runs were generally less than the precipitation differences in some of the model
347 ensembles with no soil moisture change indicating the soil moisture impacts were not significant.
348 Here it was shown that total precipitation was not substantially affected by non-uniform soil
349 moisture increases. This study also confirms that WRF has low skill for high resolution forecasts
350 for convection, and the alternate soil moisture initializations do not change this.

351 A possible limitation of this study is that NARR data were used as initial and boundary
352 conditions and not a higher resolution dataset such as those used by *Trier et al.* [2004] and *Case*
353 *et al.* [2011], which found that the high resolution initial soil moisture data improved convection
354 forecasts. Although SMOS data were regridded to a 4 km horizontal resolution, due to the lower
355 resolution of the satellite, some degree of spatial autocorrelation was expected among the pixels.
356 This indicates that some of the fine scale initial soil moisture variations in the SMOS runs may

not be accurate. SMAP, which is designed to measure soil moisture at a higher horizontal resolution, will likely be able to pick up on these fine scale features better than SMOS and theoretically be more useful in these types of cases. Another important issue is the fact that the soil moisture magnitude differences between CONTROL-Run and SMOS-Run, and CONTROL + 0.10-Run and SMOS + 0.10-Run were minimal. However, this work was more concerned with the spatial distribution of soil moisture rather than the magnitude. While it would be interesting to determine satellite biases with respect to in-situ observations, there are simply not enough available. Even within Oklahoma, the mean station density of the Oklahoma Mesonet is one station per 1,510 km^2, calculated by dividing the geographic size of Oklahoma (181,186 km^2) by the number of stations available (120), This value is greater than the area of a grid cell in the outer most WRF nest (1,296 km^2). *Collow et al.* [2012] used observation sites clustered close together to deduce a mean SMOS bias of 0.1 m^3/m^3, which is equivalent to the NARR mean bias discovered in *Collow et al.* [2014]. This supports Figure 3, which shows little change in magnitude between the NARR and SMOS mean soil moisture over the primary evaluation region. A final concern would be the number of available cases to work with for this study. In order to qualify as a case, a satellite pass needed to occur at 00 UTC. This only occurred 13% of the time over all of the days in June through August in 2010 and 2011. Even if all days were considered, no matter the precipitation, the value would increase to only 15%.

This study showed strong relationships between initial soil moisture perturbations and the resultant 2 m temperature and dewpoint. *Frye and Mote* [2010] note that dewpoint changes impact convective available potential energy more than temperature changes, which would result in a greater probability of convection. However, studies such as *DeAngelis et al.* [2010] and *Collow et al.* [2014] found that the temperature and humidity effects cancel each other out

resulting in minimal local impacts on convection. The idea of a positive feedback between soil moisture and precipitation is proposed in numerous studies [*Eltahir,* 1998; *Koster et al.,* 2006], but so is the theory of a negative feedback [*Findell and Eltahir,* 2003; *Taylor and Ellis,* 2006]. It is obvious that there are many competing factors relating to soil moisture and atmosphere interactions and that there is still much uncertainty illustrating the need for better soil moisture measurements and continued remote sensing missions to provide a global analysis of soil moisture.

Although the methods employed in this study used several assumptions and approximations, results found were still significant and have implications for future land surface sensitivity studies using the WRF model. Our main findings are presented below.

1. Using a different soil moisture initialization dataset such as that based on SMOS had little to no impact on the skill of WRF to forecast the spatial scale of precipitation over the US Great Plains. *ETS* generally remained below 0.4 in all runs reflecting low skill for each model run. Total precipitation amounts were, on average, slightly higher in the + 0.10 soil moisture runs.

2. A strong anti-correlation existed between the initial soil moisture and the resultant 2 m temperature. There was also generally a moderate correlation between the initial soil moisture and 2 m dewpoint.

3. SMOS data showed some promise in terms of its usefulness for improving numerical weather forecasting models as there were some locations that saw significant improvements in temperature and humidity forecasts relative to control runs. However, more robust data assimilation methods will be needed to confirm these results.

401 **Acknowledgments.** This work has been supported by NASA Grant NNX09AJ99G and the
402 Brookhaven National Laboratory (BNL) Laboratory Directed Research and Development
403 Program. Calculations were performed at the NCAR Wyoming Supercomputing Center, which
404 is supported by NSF. We thank Yann Kerr for providing us with the reprocessed SMOS soil
405 moisture dataset used in this study. NARR data used in this study are available for download at
406 http://rda.ucar.edu/datasets/ds608.0/.

5. References

Bitar, A. A., D. Leroux, and Y. H. Kerr (2012), Evaluation of SMOS soil moisture products over continental U.S. using the SCAN/SNOTEL network, *IEEE Trans. Geosci. Remote Sens.*, *50*(5), 1572-1586.

Case, J. L., S. V. Kumar, J. Srikishen, and G. J. Jedlovec (2011), Improving numerical weather predictions of summertime precipitation over the southeastern United States through a high-resolution initialization of the surface state, *Weather Forecasting*, *26*, 785-807, doi: 10.1175/2011WAF2222455.1.

Chang, J.-T., and P. J. Wetzel (1991), Effects of spatial variations of soil moisture and vegetation on the evolution of a prestorm environment: A numerical case study. *Mon. Wea. Rev.*, *119*, 1368–1390, doi: 10.10175/1520-0493(1991)119<1368:EOSVOS>2.0.CO;2.

Charpentier, M. A., and P. M. Groffman (1992), Soil moisture variability within remote sensing pixels, *J. Geophys. Res.*, *97*(D17), 18,987-18,995.

Clark, C. A., and R. W. Arritt (1995), Numerical simulations of the effect of soil moisture and vegetation cover on the development of deep convection, *J. Appl. Meteorol*, *34*, 2029-2045.

Collow, T. W., A. Robock, J. B. Basara, and B. G. Illston (2012), Evaluation of SMOS retrievals of soil moisture over the central United States with currently available in-situ observations, *J. Geophys. Res.*, *117*, D09113, doi: 10.1029/ 2011JD017095.

Collow, T. W., A. Robock, and W. Wu (2014), Influences of Soil Moisture and Vegetation on Convective Precipitation Forecasts over the United States Great Plains, *J. Geophys. Res.*, in press, doi: 10.1002/2014JD021454.

Crow, W. T., et al. (2012), Upscaling sparse ground-based soil moisture observations for the validation of coarse-resolution satellite soil moisture products, *Rev. Geophys, 50*(2), RG2002, doi:10.1029/2011RG000372.

DeAngelis, A., F. Dominguez, Y. Fan, A. Robock, M. D. Kustu, and D. Robinson (2010) Observational evidence of enhanced precipitation due to irrigation over the Great Plains of the United States. *J. Geophys. Res., 115,* D15115, doi:10.1029/2010JD013892.

Done, J., C. A. Davis, and M. Weisman (2004), The next generation of NWP: explicit forecasts of convection using the weather research and forecasting model, *Atmos. Sci. Lett, 5,* 110-117, doi: 10.1002/asl.72.

Draper, C. S., R. H. Reichle, G. J. M. De Lannoy, and Q. Liu (2012), Assimilation of passive and microwave soil moisture retrievals, *Geophys. Res. Lett., 39,* L04401, doi: 10.1029/2011GL050655.

Dudhia, J. (1989), Numerical study of convection observed during the Winter Monsoon Experiment using a mesoscale two dimensional model, *J. Atmos. Sci., 46,* 3077–3107.

Ek, M. B., K. E. Mitchell, Y. Lin, E. Rogers, P. Grunmann, V. Koren, G. Gayno, and J. D. Tarpley (2003), Implementation of Noah land surface model advances in the National Centers for Environmental Prediction operational mesoscale Eta Model, *J. Geophys. Res, 108,* 8851, doi:10.100.1029/2002JD003296.

Eltahir, E. A. (1998), A soil moisture–rainfall feedback mechanism: 1. Theory and observations, *Water Resour. Res., 34*(4), 765–776, doi:10.1029/97WR03499.

Entekhabi, D., et al. (2010), The soil moisture active passive (SMAP) mission, *Proc. IEEE, 98*(5), 704-716.

Findell, K.L., and E. A. Eltahir (2003), Atmospheric controls on soil moisture-boundary layer interactions. Part II: Feedbacks within the continental United States, *J. Hydrometeor., 4*, 570-583.

Frye, J. D., and T. L. Mote (2010), The synergistic relationship between soil moisture and the low-level jet and its role on the prestorm environment over the Southern Great Plains, *J. Appl. Meteor. Climatol., 49,* 775-791, doi: 10.10175/2009JAMC 2146.1.

Gesch, D., B., K. L. Verdin, and S. K. Greenlee (1999), New land surface digital elevation model covers the Earth, *EOS Trans. Am. Geophys. Union, 80*(6), 69-70.

Hong, S.-Y. and J.-O. J. Lim (2006), The WRF single-moment 6-class microphysics scheme (WSM6), *J. Korean Meteor. Soc.*, *42*(2), 129-151.

Imaoka, K., et al. (2010), Global change observation mission (GCOM) for monitoring carbon, water cycles, and climate change, *Proc. IEEE.*, *98*(5), 717-734, doi: 10.1109/JPROC.2009.2036869.

Jackson, T. J., et al. (2012), Validation of Soil Moisture and Ocean Salinity (SMOS) soil moisture over watershed networks in the U.S., *IEEE Trans. Geosci. Remote Sens.*, *50*(5), 1530-1543, doi: 10.1109/TGRS.2011.2168533.

Kain, J. S., et al. (2008), Some practical considerations regarding horizontal resolution in the first generation of operational convection-allowing NWP. *Wea. Forecasting*, *23*, 931–952. doi: 10.10175/WAF2007106.1.

Kerr Y. H., P. Waldteufel, J.-P. Wigneron, J.-M. Martinuzzi, J. Font, and M. Berger (2001), Soil moisture retrieval from space: The Soil Moisture and Ocean Salinity (SMOS) mission, *IEEE Trans. Geosci. Remote Sens.*, *39*, 1729-1735.

472 Koster, R. D., et al. (2006), GLACE: The global land-atmosphere coupling experiment. Part I:
473 overview, *J. Hydrometeor.*, *7*, 590-610.
474 Kumar, S. V., R. H. Reichle, R. D. Koster, W. T. Crow, C. D. Peters-Lidard (2009), Role of
475 subsurface physics in the assimilation of surface soil moisture observations. *J. Hydrometeor*,
476 *10*, 1534–1547, doi: 10.1175/2009JHM1134.1.
477 Lanicci, J. M., T. N. Carlson, and T. T. Warner (1987), Sensitivity of the Great Plains severe
478 storm environment to soil moisture distribution, *Mon Wea. Rev.*, *115*, 2660-2673.
479 Lin, Y., and K. E. Mitchell (2005), The NCEP stage II/IV hourly precipitation analyses:
480 Development and applications, paper presented at 19th Conf. on Hydrology, Am. Meteorol.
481 Soc., San Diego, CA, 1.2.
482 Mahfouf, J.-F., E. Richard, P. Mascart (1987), The influence of soil and vegetation on the
483 development of mesoscale circulations. *J. Climate Appl. Meteor.*, *26*, 1483–1495.
484 Mellor G. L., and T. Yamada (1982), Development of a turbulence closure model for
485 geophysical fluid problems, *Rev. Geophys.*, *20(4)*, 851–875.
486 Mesinger, F., et al. (2006), The North American Regional Reanalysis, *Bull. Am. Meteorol. Soc*.,
487 *87*, 343-360, doi: 10.10175/BAMS-87-3-343.
488 Mlawer, E. J., S. J. Taubman, P. D. Brown, M. J. Iacono, and S. A. Clough (1997), Radiative
489 transfer for inhomogeneous atmosphere: RRTM, a validated correlated-k model for the
490 longwave, *J. Geophys. Res.*, *102*(D14), 16,663–16,682.
491 Njoku, E. G., T. J. Jackson, V. Lakshmi, T. K. Chan, and S. V. Nghiem (2003), Soil moisture
492 retrieval from AMSR-E, *IEEE Trans. Geosci. Remote Sens.*, *41*, 215-229.

493 Ookouchi, Y., M. Segal, R. C. Kessler, R. A. Pielke (1984), Evaluation of soil moisture effects
494 on the generation and modification of mesoscale circulations. *Mon. Wea. Rev., 112*, 2281–
495 2292.
496 Pielke, R. A. and X. Zeng (1989), Influence on severe storm development of irrigated land.
497 *National Weather Digest, 14*(2), 16-17.
498 Reichle, R. H. and R. D. Koster (2004), Bias reduction in short records of satellite soil moisture,
499 *Geophys. Res. Lett., 31*, L19501, doi:10.1029/2004GL020938
500 Reichle, R. H. (2008), Data assimilation methods in Earth sciences, *Adv. Water Resour., 31*,
501 1411-1418.
502 Sabater, J. M., L. Jarlan, J.-C. Calvet, and F. Bouyssel (2006), From near-surface to root-zone
503 soil moisture using different assimilation techniques, *J. Hydrometeor., 8*, 194-206.
504 Sabater, J. M., A. Fouilloux and P. de Rosnay (2012), Technical implementation of SMOS data
505 in the ECMWF Integrated Forecasting System, *IEEE Trans. Geosci. Remote Sens.*, *9*(2), doi:
506 10.1109/LGRS.2011.2164777.
507 Schneider, S., Y. Wang, W. Wagner, and J. Mahfouf (2013), Impact of ASCAT soil moisture
508 assimilation on regional precipitation forecasts: A case study for Austria, *Mon. Wea. Rev.*, in
509 press, doi:10.1175/MWR-D-12-00311.1.
510 Skamarock, W. C., et al. (2008), A description of the Advanced Research WRF version 3,
511 NCAR Technical Note, NCAR/TN-475+STR, 125 pp., (Available online at
512 http://www.mmm.ucar.edu/wrf/users/docs/arw_v3.pdf).
513 Taylor, C. M., and R. J. Ellis (2006), Satellite detection of soil moisture impacts on convection at
514 the mesoscale, *Geophys. Res. Lett., 33*(3), L03404, doi: 10.1029/2005GL025252.

515 Trier, S. B., F. Chen, and K. W. Manning (2004), A study of convection initiation in a mesoscale
516 model using high resolution land surface initial conditions, *Mon. Wea. Rev., 132*, 2954-2976.
517 Vinnikov, K. Y., A. Robock, S. Qiu, J. K. Entin, M. Owe, B. J. Choudhury, S. E. Hollinger, and
518 E. G. Njoku (1999), Satellite remote sensing of soil moisture in Illinois, USA, *J. Geophys.*
519 *Res., 104*, 4145-4168.
520 Weisman, M. L., C. Davis, W. Wang, K. W. Manning, and J. B. Klemp (2008), Experiences with
521 0-36-h explicit convective forecasts with the WRF-ARW model, *Wea. Forecasting, 23*, 407-
522 437, doi: 10.1175/2007WAF2007005.1.
523 Zhao, L., K. Yang, J. Qin, Y. Chen, W. Tang, H. Lu, and Z.-L. Yang (2014), The scale-
524 dependence of SMOS soil moisture accuracy and its improvement through land data
525 assimilation in the central Tibetan Plateau, *Remote Sens. Environ.*, *152*, 345-355, doi:
526 10.1016/j.rse.2014.07.005.

527 **Table 1.** Mean total precipitation (mm) over the evaluation domain from 18 UTC through 06
528 UTC the next day for all cases in this study (dates presented in mm-dd-yyyy format). The last
529 row shows the mean over all cases.

	CONTROL-Run	CONTROL + 0.10-Run	SMOS-Run	SMOS + 0.10-Run	NCEP Stage IV
23 Jun 2010	0.64	0.87	0.93	0.86	2.09
06 Jul 2010	4.28	4.86	4.19	5.15	3.75
11 Jul 2010	0.38	0.69	0.76	1.19	3.62
24 Jul 2010	4.02	5.03	4.16	5.29	6.75
16 Aug 2010	3.14	4.27	2.96	4.44	3.26
10 Jun 2011	1.54	2.25	1.38	1.83	1.18
28 Jun 2011	1.71	1.36	1.59	0.86	1.60
29 Jul 2011	0.71	1.26	0.65	1.04	1.34
03 Aug 2011	1.99	2.36	1.55	2.05	3.17
16 Aug 2011	0.29	0.19	0.44	0.20	1.34
MEAN	**1.87**	**2.31**	**1.86**	**2.29**	**2.97**

530

Table 2: Spatial correlation coefficients between soil moisture differences and maximum and mean 2 m temperature and dewpoint changes for all cases for the period 18 UTC through 06 UTC the next day. Correlations are calculated on the inner most WRF grid and grid cells with precipitation were filtered out. The +0.00 columns represent the changes from CONTROL-Run to SMOS-Run and the +0.10 columns denote the changes from CONTROL + 0.10-Run to SMOS + 0.10-Run. The mean and standard deviation is calculated using both the +0.00 and +0.10 columns for temperature and dewpoint.

	Max 2 m Temperature	**Mean 2 m Temperature**	**Max 2 m Dewpoint**	**Mean 2 m Dewpoint**
	+0.00 | +0.10	**+0.00 | +0.10**	**+0.00 | +0.10**	**+0.00 | +0.10**
23 Jun 2010	-0.77 | -0.77	0.65 | 0.71	0.52 | 0.59	0.65 | 0.62
06 Jul 2010	-0.83 | -0.76	0.80 | 0.68	0.17 | 0.23	0.66 | 0.56
11 Jul 2010	-0.74 | -0.78	0.60 | 0.76	0.47 | 0.50	0.57 | 0.62
24 Jul 2010	-0.83 | -0.86	0.77 | 0.83	0.57 | 0.79	0.67 | 0.79
16 Aug 2010	-0.74 | -0.80	0.61 | 0.67	0.45 | 0.58	0.52 | 0.65
10 Jun 2011	-0.76 | -0.70	0.47 | 0.57	0.58 | 0.40	0.61 | 0.50
28 Jun 2011	-0.56 | -0.64	0.42 | 0.54	0.34 | 0.40	0.42 | 0.43
29 Jul 2011	-0.82 | -0.86	0.50 | 0.70	0.37 | 0.66	0.69 | 0.80
03 Aug 2011	-0.62 | -0.74	0.33 | 0.59	0.51 | 0.41	0.55 | 0.61
16 Aug 2011	-0.57 | -0.64	0.47 | 0.56	0.17 | 0.37	0.30 | 0.42
MEAN	**-0.74**	**-0.61**	**0.45**	**0.58**
STANDARD DEVIATION	**0.09**	**0.13**	**0.16**	**0.13**

539 **Table 3.** Mean WRF 2 m temperature bias (°C) with respect to Oklahoma Mesonet with
540 precipitation filtered (WRF minus Mesonet). Max columns denote the bias from the maximum 2
541 m temperature between 18 UTC and 06 UTC the next day and the mean columns represent the
542 bias of the average temperature over the same time interval. Significant differences at the 95%
543 confidence interval with respect to control are highlighted red. An asterisk (*) denotes an
544 improvement with respect to control.

	CONTROL-Run Max | Mean	CONTROL + 0.10-Run Max | Mean	SMOS-Run Max | Mean	SMOS + 0.10-Run Max | Mean
23 Jun 2010	3.5 | 2.4	1.0* | 0.8*	3.4* | 2.3*	0.8* | 0.5*
11 Jul 2010	4.1 | 3.2	2.0* | 1.9*	2.0* | 1.0*	1.0* | 1.1*
24 Jul 2010	4.0 | 4.0	1.5* | 1.9*	4.7 | 4.3	2.0* | 2.3*
16 Aug 2010	2.6 | 2.0	0.1* | 0.0*	1.7* | 0.8*	-0.4* | -0.6*
10 Jun 2011	2.6 | 0.9	-0.4*| -0.5*	2.9 | 0.8*	-0.2* | -0.5*
28 Jun 2011	2.3 | 1.0	-0.9*| -0.6*	3.6 | 1.1	-0.1* | -0.3*
29 Jul 2011	0.4 | 0.4	-1.6 | -1.6	0.6 | 0.2*	-1.1 | -1.3
03 Aug 2011	1.4 | 1.0	-1.1* | -0.7*	2.1 | 0.7*	-0.3* | 0.2*
16 Aug 2011	2.4 | 2.2	-0.1* | 0.3*	2.0* | 1.6*	-0.2* | 0.1*
MEAN	**2.6 | 1.9**	**0.1* | 0.2***	**2.6 | 1.4***	**0.2* | 0.2***
STANDARD DEVIATION	**1.2 | 1.2**	**1.2 | 1.2**	**1.2 | 1.2**	**0.9 | 1.1**

545

546 **Table 4.** Same as Table 3 except for maximum 2 m dewpoint (°C)

	CONTROL-Run Max | Mean	CONTROL + 0.10-Run Max | Mean	SMOS-Run Max | Mean	SMOS + 0.10-Run Max | Mean
23 Jun 2010	-1.7 | -2.0	0.8* | 0.9*	-1.5* | -1.9*	0.6* | 0.6*
11 Jul 2010	-2.3 | -3.0	-0.3* | -0.4*	-0.6* | -1.4*	0.8* | 0.8*
24 Jul 2010	-2.5 | -3.3	-0.4* | -0.5*	-2.7 | -3.9	-0.7* | -1.0*
16 Aug 2010	-1.5 | -2.2	0.7* | 0.5*	-0.4* | -1.4*	1.4* | 0.9*
10 Jun 2011	-1.9 | -2.2	0.1* | 0.0*	-2.5 | -2.8	-0.1* | -0.4*
28 Jun 2011	-0.2 | -1.7	1.9 | 2.0	-0.6 | -2.7	1.1 | 0.9*
29 Jul 2011	0.5 | 0.8	3.0 | 3.5	0.5 | 0.6*	2.5 | 2.8
03 Aug 2011	-0.8 | -1.3	3.1 | 2.5	-1.1 | -1.8	1.1 | 1.0*
16 Aug 2011	-1.8 | -1.3	1.2* | 1.6	-0.8* | -0.4*	1.7* | 2.1
MEAN	**-1.4 | -1.8**	**1.1* | 1.1***	**-1.2* | -1.7***	**0.9* | 0.9***
STANDARD DEVIATION	**1.0 | 1.2**	**1.3 | 1.4**	**1.0 | 1.3**	**0.9 | 1.1**

547

548 **Figures**

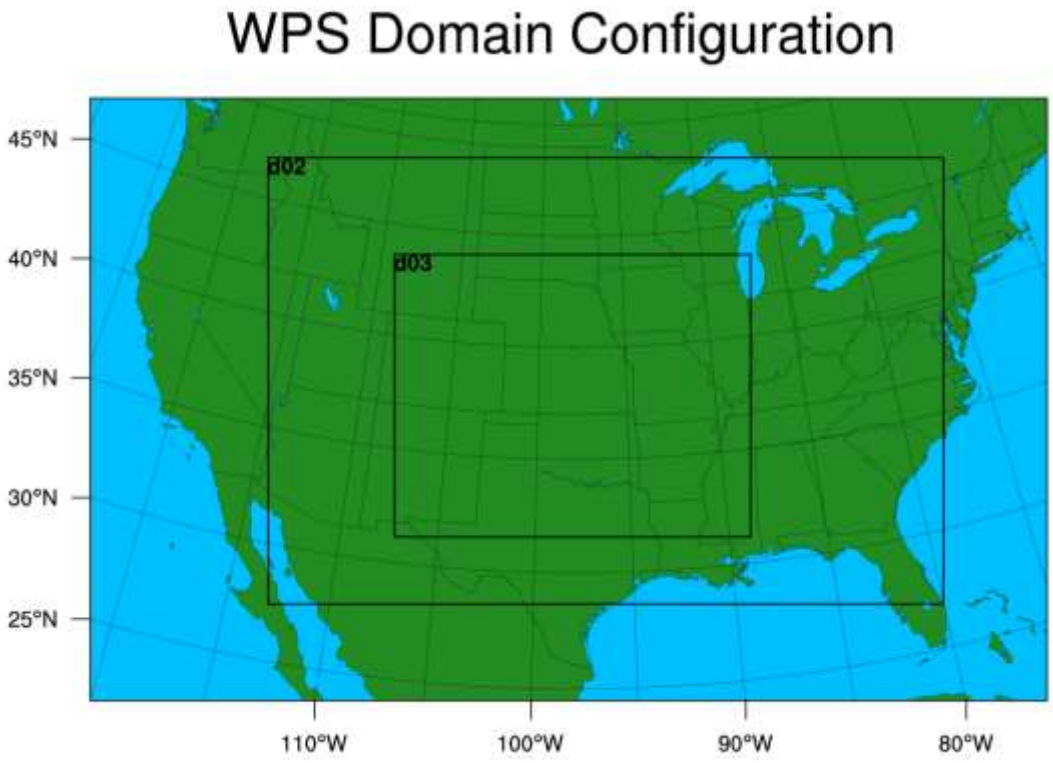

549
550 **Figure 1.** Domain nests used for WRF experiments generated by the WRF Pre-processing
551 System (WPS). Outer domain (the entire image) was nudged at the edge by the NARR data and
552 run at a grid resolution of 36 km. Domain d02 was run at 12 km resolution. Results shown in
553 paper encompass the inner domain, d03, run at a 4 km resolution.

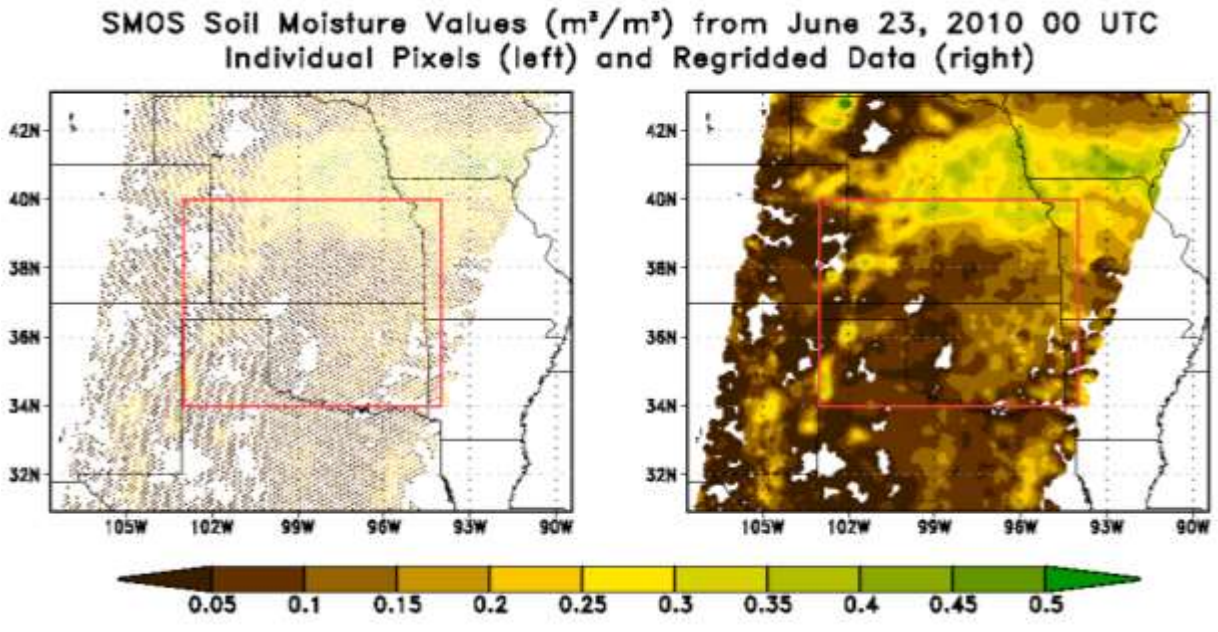

554

555 **Figure 2.** Individual SMOS soil moisture (m^3/m^3) pixels (left) and regridded SMOS soil

556 moisture (m^3/m^3; right) for June 23, 2010 00 UTC. Red box represents the evaluation domain.

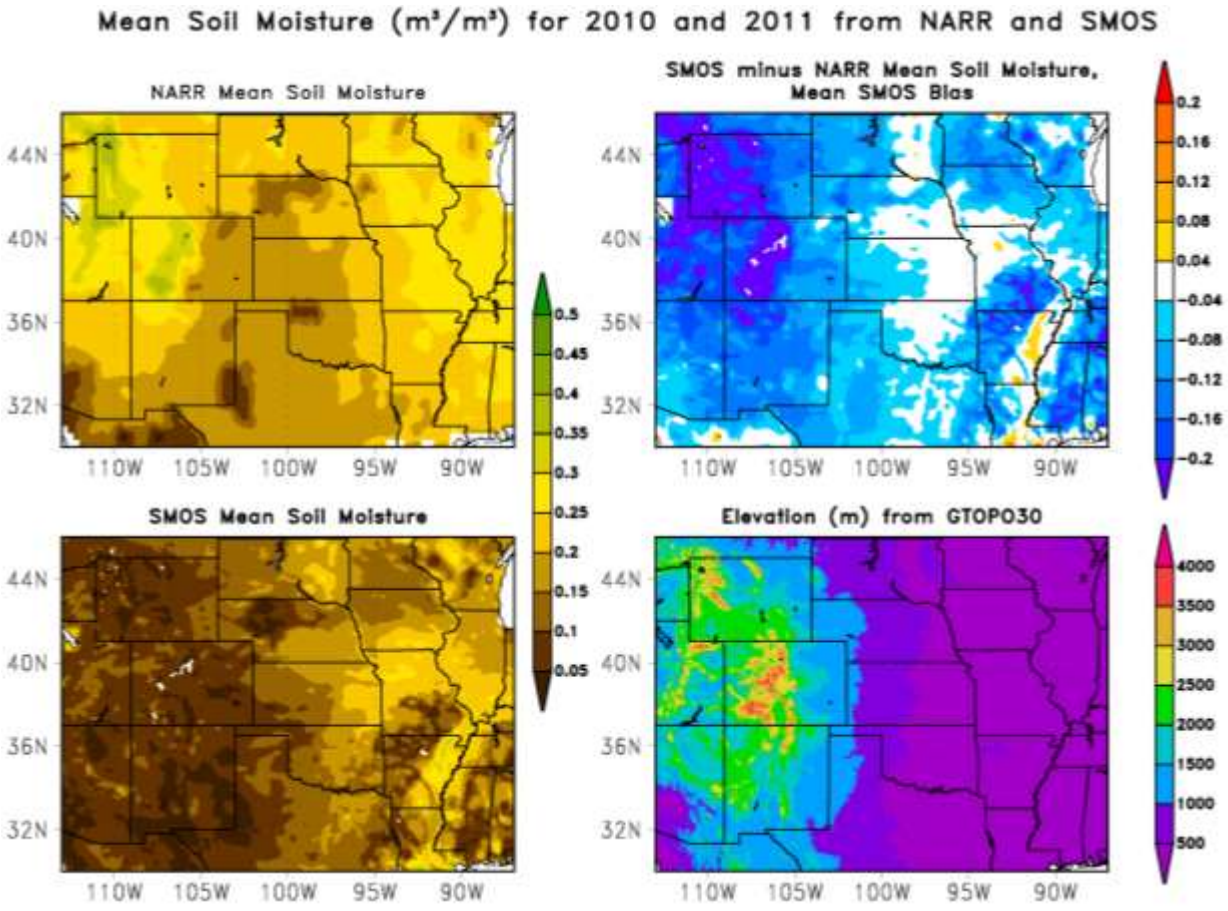

Figure 3. Mean soil moisture (m^3/m^3) from March through November 2010 and 2011 for NARR (top left) and SMOS (bottom right). Difference between SMOS and NARR or the SMOS bias is also plotted (top right) with elevation (m) from GTOPO30 plotted in the bottom right for reference.

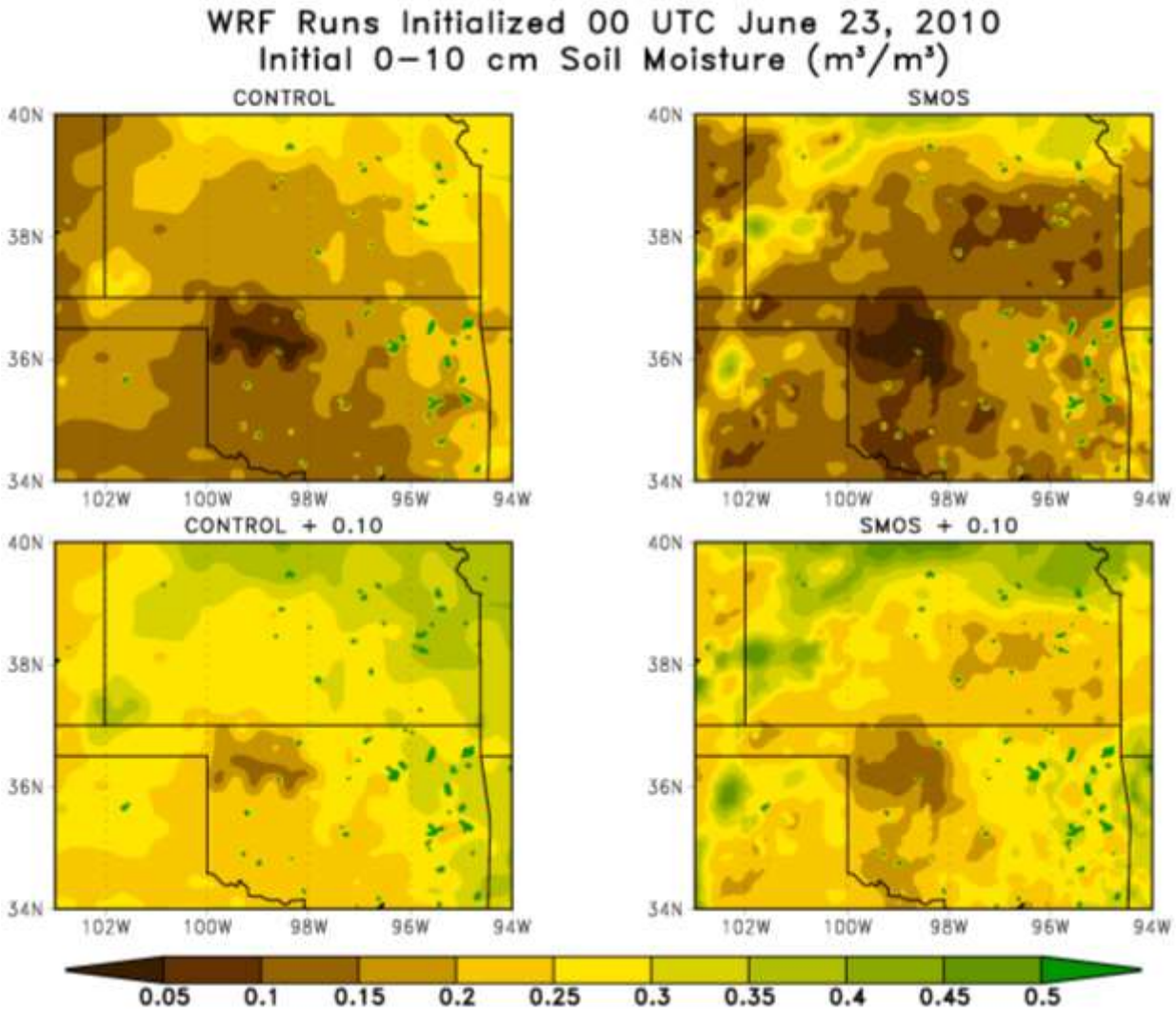

Figure 4. Initial 0-10 cm depth soil moisture (m^3/m^3) for each of the four WRF simulations starting at 00 UTC June 23, 2010. CONTROL-Run (top left), SMOS-Run (top right), CONTROL+ 0.10-Run (bottom left) and SMOS + 0.10-Run (bottom right). Plot area represents the evaluation domain.

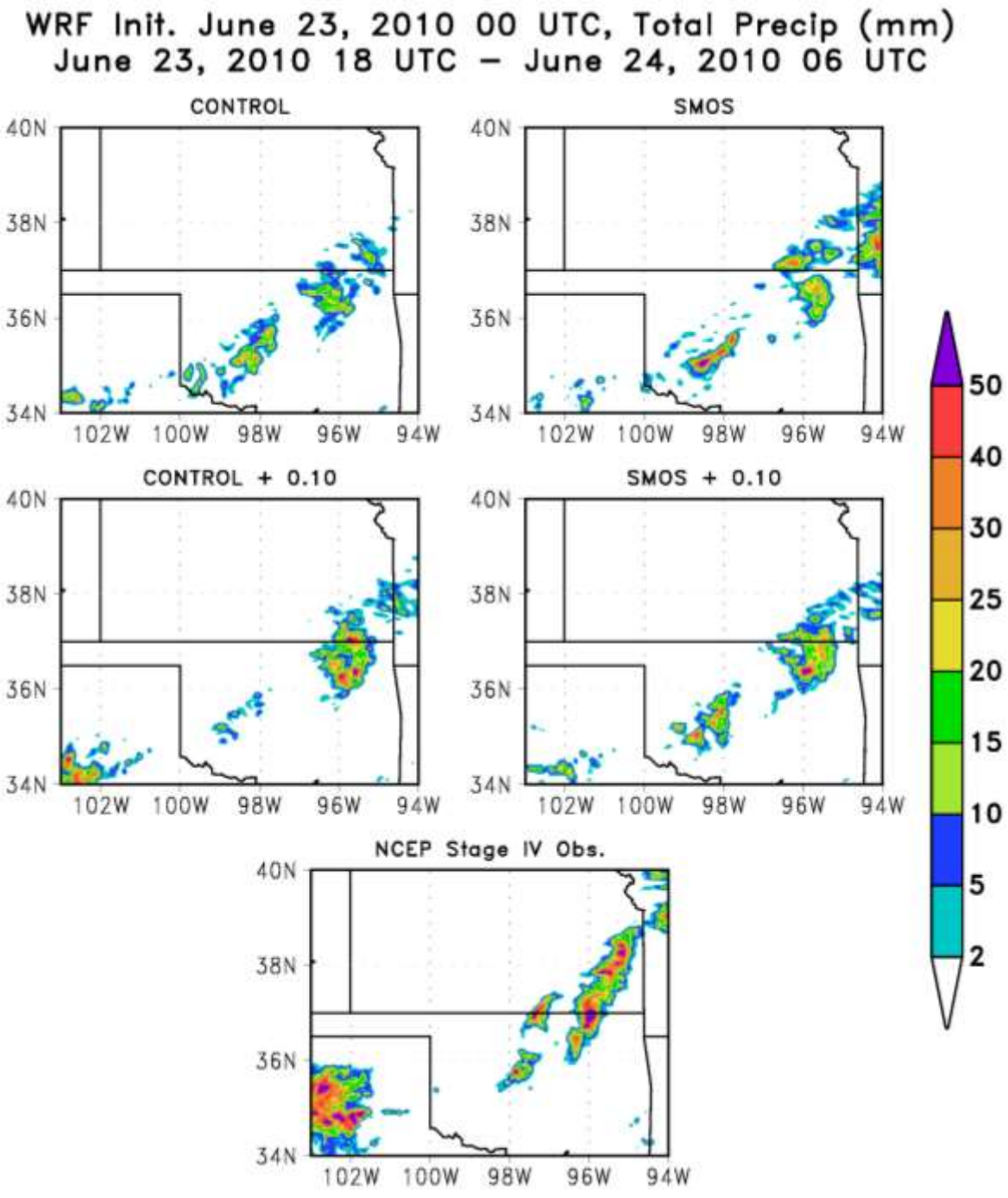

Figure 5. Total WRF modeled and observed precipitation (mm) from 18 UTC June 23, 2010 through 06 UTC June 24, 2010. Clockwise from top left; CONTROL-Run, SMOS-Run, SMOS + 0.10-Run, NCEP Stage IV Observations, CONTROL + 0.10-Run. Plot area represents the evaluation domain.

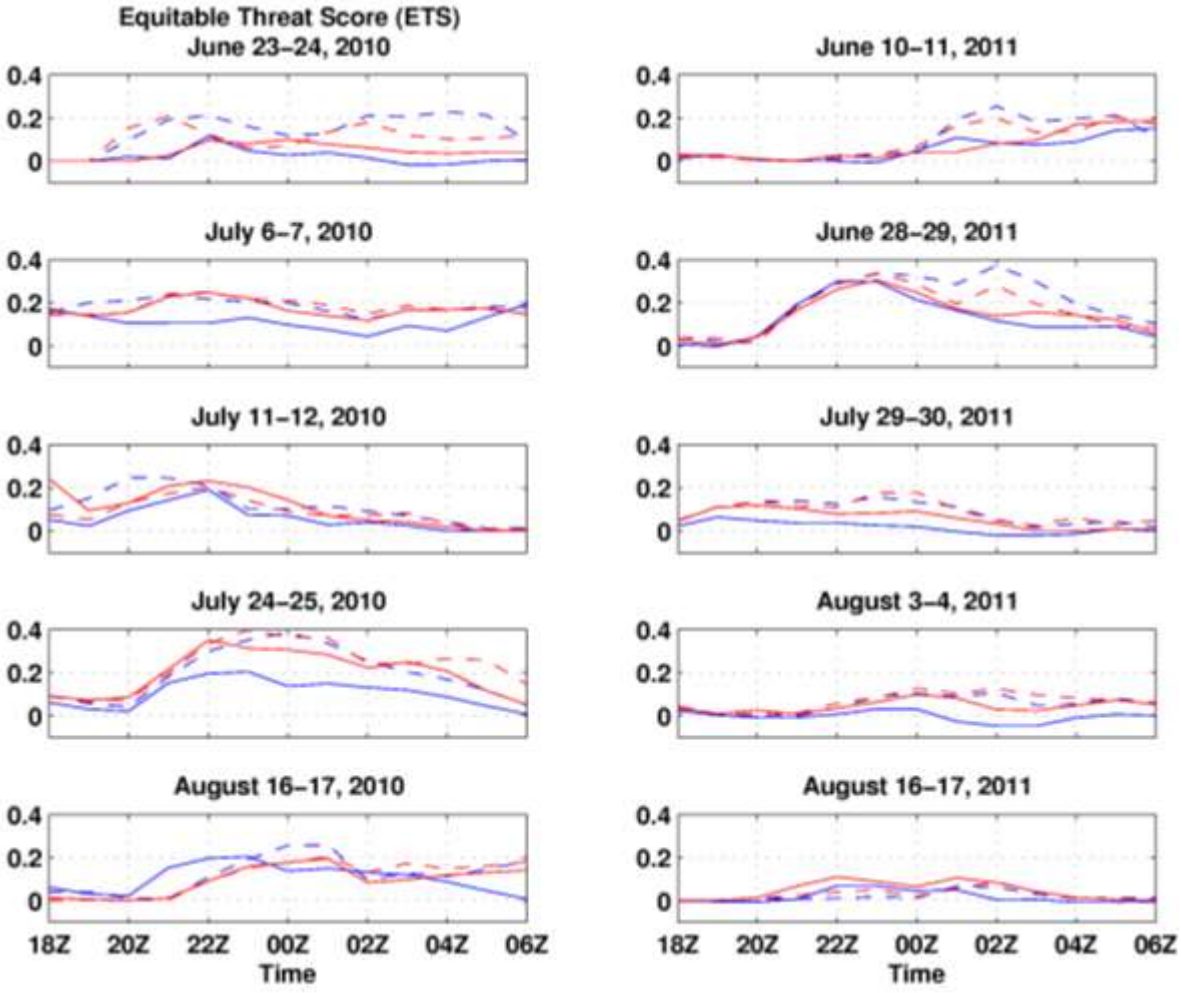

573

574 **Figure 6:** ETS of WRF precipitation occurrence forecasts across the inner domain from runs
575 with different initial soil moisture for all cases. Any amount of precipitation is considered for
576 verification. Blue lines represent CONTROL-Run and CONTROL+0.10-Run, and red lines
577 denote SMOS-Run and SMOS+0.10--Run. Solid lines and Dashed lines represent no additional
578 soil moisture and + 0.10 m^3/m^3 additional soil moisture respectively.

579

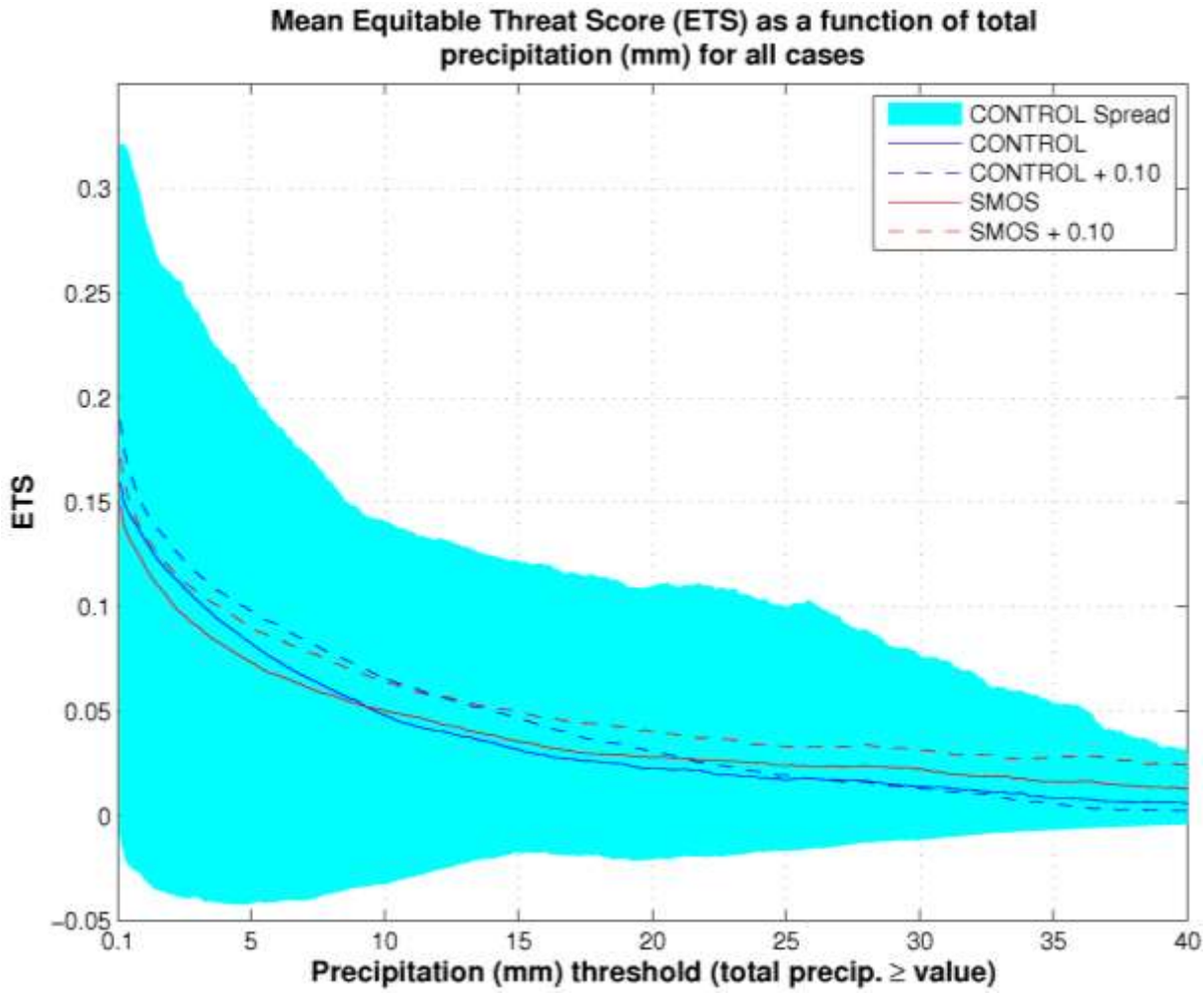

Figure 7. Mean ETS as a function of forecasted total precipitation from all cases. The shaded region represents the spread from the CONTROL-Run and CONTROL+0.10-Run for each case. ETS was calculated using hits defined as grid cells with precipitation amounts greater than or equal to a certain threshold (x-axis) and misses with precipitation amounts less than that same threshold.

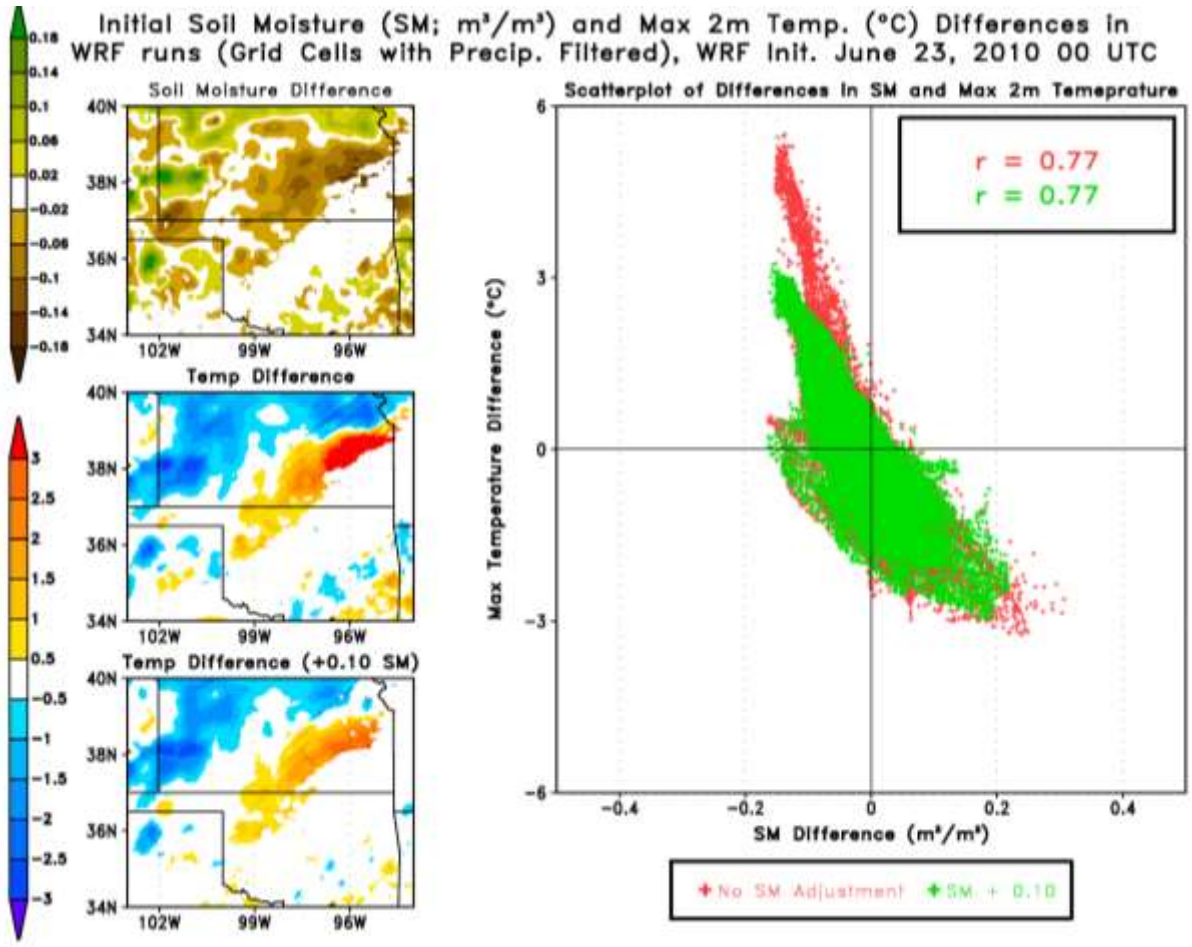

Figure 8. Left column from top to bottom: Difference in initial soil moisture between SMOS-Run and CONTROL-Run (SMOS-Run minus CONTROL-Run) for June 23, 2010 case; Difference in maximum 2 m temperature between SMOS-Run and CONTROL-Run for the period 18 UTC June 23 through 06 UTC June 24; Difference in maximum 2 m temperature between SMOS + 0.10-Run and CONTROL + 0.10-Run for the period 18 UTC June 23 through 06 UTC June 24. Right: Scatterplot of soil moisture differences vs. maximum 2 m temperature differences with red marks representing CONTROL-Run vs. SMOS-Run and the green marks CONTROL + 0.10-Run and SMOS + 0.10-Run. Correlation coefficients are shown in the upper right.